The E3 ubiquitin ligase midline 1 promotes allergen and rhinovirus-induced asthma by inhibiting protein phosphatase 2A activity

Adam Collison[1,2,10], Luke Hatchwell[1,2,10], Nicole Verrills[3], Peter A B Wark[2,4], Ana Pereira de Siqueira[1,2], Melinda Tooze[2,4], Helen Carpenter[3], Anthony S Don[5], Jonathan C Morris[6], Nives Zimmermann[7], Nathan W Bartlett[8], Marc E Rothenberg[7], Sebastian L Johnston[8], Paul S Foster[2] & Joerg Mattes[1,2,9]

© 2013 Nature America, Inc. All rights reserved.

Allergic airway inflammation is associated with activation of innate immune pathways by allergens. Acute exacerbations of asthma are commonly associated with rhinovirus infection. Here we show that, after exposure to house dust mite (HDM) or rhinovirus infection, the E3 ubiquitin ligase midline 1 (MID1) is upregulated in mouse bronchial epithelium. HDM regulates MID1 expression in a Toll-like receptor 4 (TLR4)– and tumor necrosis factor–related apoptosis-inducing ligand (TRAIL)-dependent manner. MID1 decreases protein phosphatase 2A (PP2A) activity through association with its catalytic subunit PP2Ac. siRNA-mediated knockdown of MID1 or pharmacological activation of PP2A using a nonphosphorylatable FTY720 analog in mice exposed to HDM reduces airway hyperreactivity and inflammation, including the expression of interleukin-25 (IL-25), IL-33 and CCL20, IL-5 and IL-13 release, nuclear factor (NF)κB activity, p38 mitogen-activated protein kinase (MAPK) phosphorylation, accumulation of eosinophils, T lymphocytes and myeloid dendritic cells, and the number of mucus-producing cells. MID1 inhibition also limited rhinovirus-induced exacerbation of allergic airway disease. We found that MID1 was upregulated in primary human bronchial epithelial cells upon HDM or rhinovirus exposure, and this correlated with TRAIL and CCL20 expression. Together, these findings identify a key role of MID1 in allergic airway inflammation and links innate immune pathway activation to the development and exacerbation of asthma.

Allergic airway inflammation and asthma are associated with the activation of innate and adaptive immune cells[1]. The cytokines thymic stromal lymphopoietin (TSLP), granulocyte-macrophage colony–stimulating factor (GM-CSF), IL-25, IL-33 and tumor necrosis factor–related apoptosis-inducing ligand (TRAIL) are released by bronchial epithelial cells upon allergen exposure, activating dendritic cells and promoting T helper type 2 (T_H2) cell differentiation[2–4]. T_H2 cells then release IL-13, which induces airway hyperreactivity (AHR) and mucus production in a signal transducer and activator of transcription 6 (STAT6)-dependent manner[5–8]. Respiratory infections, which are predominantly caused by rhinovirus in people with asthma, exacerbate airway inflammation and further contribute to disease burden and healthcare costs[9–11]. Some individuals with asthma have deficiencies in their antiviral epithelial response, predisposing them to exaggerated inflammatory responses[12,13]. This places the bronchial epithelium at the center of asthma pathogenesis and makes it a target for advanced therapeutics[14,15].

To identify new signaling pathways activated by allergens, we determined gene transcripts that were differentially expressed in blunt dissected airway wall tissue of wild-type (WT) mice and mice deficient for TRAIL (*Tnfsf10*$^{-/-}$) (ArrayExpress accession no. E-MEXP-2960), which are protected from ovalbumin-[4] and HDM-induced (**Supplementary Fig. 1**) allergic airway disease. Among other mRNA sequences, we found that the microtubule-associated E3 ubiquitin ligase MID1 (also known as tripartite motif-containing protein (TRIM) 18) was upregulated in WT mice sensitized and challenged with HDM (allergic mice) as compared to WT mice sensitized and challenged with normal saline only (nonallergic control mice) and allergic *Tnfsf10*$^{-/-}$ mice (**Fig. 1a**). We observed increased MID1-specific staining in allergic WT mice primarily in bronchial epithelial cells (**Fig. 1a**). TLR4 signaling is required for the development of allergic airway inflammation in response to HDM extract[16–19]. Upregulation of MID1 was attenuated in mice deficient in TLR4 (*Tlr4*$^{-/-}$) or the

[1]Experimental and Translational Respiratory Group, University of Newcastle and Hunter Medical Research Institute, Newcastle, New South Wales, Australia. [2]Priority Research Centre for Asthma and Respiratory Diseases, University of Newcastle and Hunter Medical Research Institute, Newcastle, New South Wales, Australia. [3]Discipline of Medical Biochemistry, School of Biomedical Science and Pharmacy, University of Newcastle, Newcastle, New South Wales, Australia. [4]Department of Respiratory and Sleep Medicine, John Hunter Hospital, Newcastle, New South Wales, Australia. [5]Lowy Cancer Research Centre, Prince of Wales Clinical School, University of New South Wales, Sydney, New South Wales, Australia. [6]School of Chemistry, University of New South Wales, Sydney, New South Wales, Australia. [7]Department of Pediatrics, Children's Hospital Medical Center, Division of Allergy and Immunology, University of Cincinnati, Cincinnati, Ohio, USA. [8]Section of Airway Disease Infection, National Heart and Lung Institute, Medical Research Council and Asthma UK Centre in Allergic Mechanisms of Asthma, Imperial College London, Norfolk Place, London, UK. [9]Paediatric Respiratory and Sleep Medicine Unit, Newcastle Children's Hospital, Kaleidoscope, Newcastle, New South Wales, Australia. [10]These authors contributed equally to this work. Correspondence should be addressed to J.M. (joerg.mattes@newcastle.edu.au).

Received 2 July 2012; accepted 29 November 2012; published online 20 January 2013; doi:10.1038/nm.3049

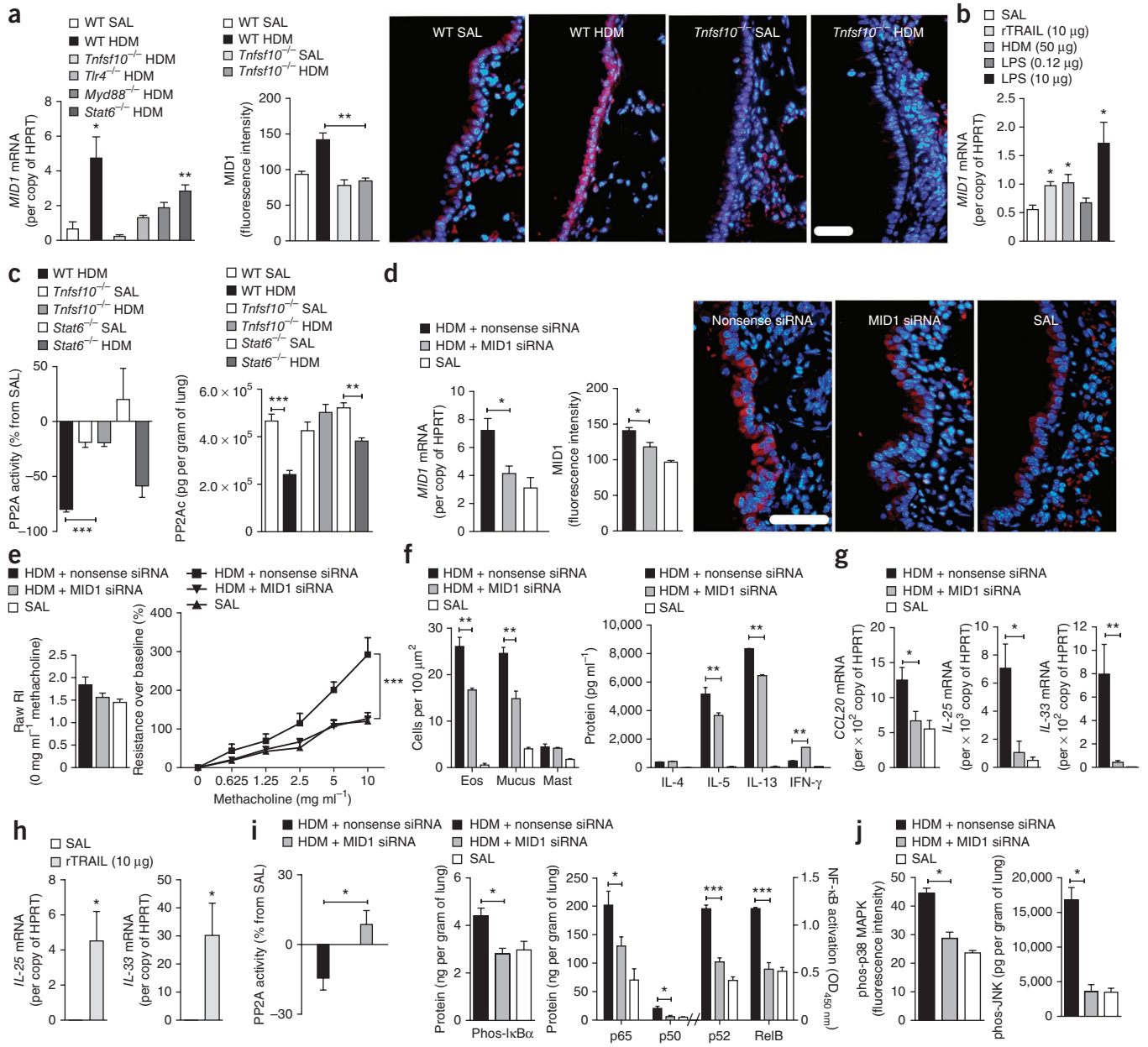

Figure 1 MID1 silencing reduces allergen-induced airway hyperreactivity, allergic inflammation and increases PP2A activity. (**a**) *MID1* mRNA and protein expression in the airway wall. Scale bar, 50 μm. MID1 (red); DNA (DAPI, blue). (**b**) *MID1* mRNA expression in naive mice 24 h after treatment with one dose of rTRAIL, house dust mite or LPS intranasally. (**c**) PP2A activity and PP2Ac protein expression in lung homogenates of nonallergic (SAL) and allergic (HDM) mice ($n = 3$–5 mice per group). (**d**) *MID1* mRNA expression and MID1 protein measured by quantification of immunofluorescence in the airway wall of SAL versus HDM mice treated intranasally with a nonsense siRNA or a MID1-targeting siRNA (MID1 siRNA) every second day during the allergen challenge period. Scale bar, 50 μm. ($n = 3$–6 mice per group). (**e**) Total lung resistance (RI) at baseline (left) and as percentage change of baseline measurement (PBS) in response to inhaled methacholine (right) ($n = 5$ or 6 mice per group). (**f**) Number of peribronchial/perivascular eosinophils, PAS-positive mucus-producing epithelial cells, and mast cells per 100 μm^2 ($n = 3$ or 4 mice per group; left) and cytokine release (right) from *in vitro* HDM-stimulated peribronchial lymph node cells (cells pooled from $n = 6$ mice per group). (**g**) *CCL20*, *IL-25* and *IL-33* mRNA expression in the airway wall normalized to HPRT. ($n = 4$–6 mice per group). (**h**) *IL-25* and *IL-33* mRNA expression in the airway wall of naive mice 24 h after treatment with one dose of rTRAIL ($n = 3$–5 mice per group). (**i,j**) PP2A activity in lung homogenates (left), levels of phosphorylated IκBα protein (middle) and activated p65 and p50 (ng per gram of lung), p52 and RelB levels (absorbance at 450 nm) (right) (n = 4–5 mice per group) (**i**). Phosphorylated JNK (phos-JNK) protein levels in lung homogenates ($n = 4$–5 mice per group) and p38 (phos-p38) MAPK protein expression measured by quantification of immunofluorescence in the airway wall. ($n = 3$ mice per group) (**j**). Results are mean ± s.e.m. $^*P < 0.05$, $^{**}P < 0.01$ and $^{***}P < 0.001$.

adaptor molecule MyD88 (*Myd88*$^{-/-}$) in response to allergen exposure as compared to allergic WT mice (**Fig. 1a**). Although mice deficient in STAT6 (*Stat6*$^{-/-}$), like *Tlr4*$^{-/-}$, *Myd88*$^{-/-}$ and *Tnfsf10*$^{-/-}$ mice, show reduced airway inflammation in response to allergen exposure[4,8,16,18], we found high MID1 expression in *Stat6*$^{-/-}$ mice sensitized and challenged with HDM (**Fig. 1a**), suggesting HDM promotes MID1 expression in a TLR4-dependent manner upstream of STAT6.

To investigate whether the induction of MID1 required pre-existing allergic inflammation, we administered one dose of either HDM, recombinant (r)TRAIL or a low or high dose of the TLR4 ligand

© 2013 Nature America, Inc. All rights reserved.

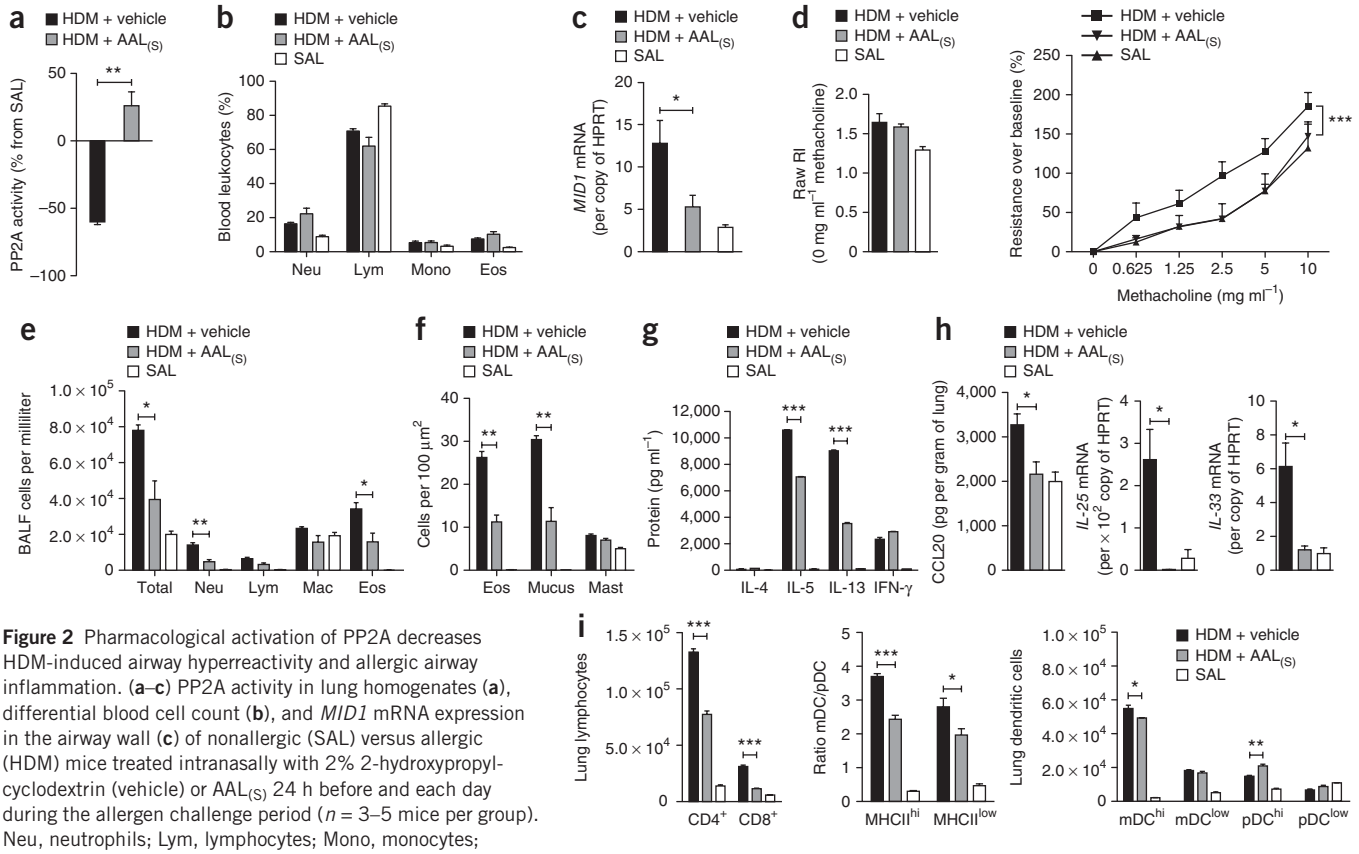

Figure 2 Pharmacological activation of PP2A decreases HDM-induced airway hyperreactivity and allergic airway inflammation. (**a**–**c**) PP2A activity in lung homogenates (**a**), differential blood cell count (**b**), and *MID1* mRNA expression in the airway wall (**c**) of nonallergic (SAL) versus allergic (HDM) mice treated intranasally with 2% 2-hydroxypropyl-cyclodextrin (vehicle) or $AAL_{(S)}$ 24 h before and each day during the allergen challenge period ($n = 3$–5 mice per group). Neu, neutrophils; Lym, lymphocytes; Mono, monocytes; Eos, eosinophils. (**d**) Total lung resistance (RI) at baseline (left) and as percentage change of baseline measurement (PBS) in response to inhaled methacholine (right) ($n = 5$–8 mice per group). (**e**) Number of cells in bronchoalveolar lavage fluid (BALF) ($n = 3$ or 4 mice per group). Mac, macrophages. (**f**) Number of peribronchial/perivascular eosinophils, PAS-positive mucus-producing epithelial cells, and mast cells per 100 μm^2 ($n = 3$ or 4 mice per group). (**g**) Cytokine release from *in vitro* HDM-stimulated peribronchial lymph node cells. (**h**) CCL20 concentration in lung homogenates, and IL-25 and IL-33 mRNA expression in the airway wall. (**i**) Number of $CD4^+$ and $CD8^+$ lymphocytes, and myeloid (m) and plasmacytoid (p) dendritic cells (DCs) determined by FACS in whole lung cell suspensions. Results are mean ± s.e.m. ($n = 3$ or 4 mice per group) for **g**–**i** . $^*P < 0.05$, $^{**}P < 0.01$ and $^{***}P < 0.001$.

© 2013 Nature America, Inc. All rights reserved.

lipopolysaccharide (LPS) intranasally to naive WT mice (**Fig. 1b**). MID1 expression was significantly upregulated in the airway wall 24 h after HDM, rTRAIL and high-dose but not low-dose LPS exposure (**Fig. 1b**).

The *MID1* gene is located at locus Xp22.3 in humans, and mutations in *MID1* have been associated with X-linked Opitz G/BBB syndrome, an inherited malformation characterized by midline defects such as cleft lip and/or palate[20]. Mutations found in individuals with Opitz syndrome disrupt transport of MID1 and migration of neural crest cells[21,22]. Beyond embryonic development, MID1 interacts with the α4 regulatory subunit of the protein phosphatase PP2A and is required for the ubiquitin-specific modification and proteasome-mediated degradation of its catalytic subunit PP2Ac[23–25]. In HDM-challenged WT and *Stat6*$^{-/-}$ mice, induction of *MID1* was associated with decreased PP2A activity and PP2Ac protein expression (**Fig. 1a**,**c**). MID1 expression, PP2A activity and PP2Ac expression remained unchanged in *Tnfsf10*$^{-/-}$ mice sensitized and challenged with HDM (**Fig. 1a**,**c**), suggesting that MID1 regulates PP2A activity upstream of STAT6 *in vivo*.

The PP2A holoenzyme is composed of three subunits; the PP2A-B subunit has multiple isoforms and confers substrate specificity, whereas PP2A-A and PP2Ac are the highly conserved scaffolding and catalytic subunits, respectively[26]. PP2A is the most abundantly expressed protein phosphatase and has been shown to dephosphorylate mitogen-activated protein kinases (MAPKs) and inhibitor of κBα (IκBα) protein, thereby limiting p38 MAPK, c-Jun N-terminal kinase (JNK) and nuclear factor-κB (NF-κB) activity [26–29]. p38 MAPK signaling activity is high in the airway wall of individuals with severe asthma[30,31] and promotes airway inflammation in mice[32,33], whereas NF-κB has a key role in T_H2-mediated allergic airway disease[34]. Dephosphorylation of JNK by PP2A has been shown to regulate glucocorticoid receptor nuclear translocation, which may be relevant for steroid-resistant asthma[35].

To assess the role of MID1 in allergic airway disease, we reduced MID1 expression by siRNA in sensitized mice 24 h before the first challenge with HDM and then every second day during challenge to levels observed in nonallergic mice (**Fig. 1d**). MID1 silencing attenuated AHR (**Fig. 1e**), reduced the accumulation of eosinophils in the lungs and the number of Alcian blue–periodic acid–Schiff (PAS)-positive mucus-producing epithelial cells (**Fig. 1f**), reduced IL-5 and IL-13 release from *ex vivo* HDM-stimulated lymph node cells isolated from the draining lymph nodes of the lungs (**Fig. 1f**), and lowered mRNA expression of CCL20, IL-25 and IL-33 (**Fig. 1g**) but not of TSLP, GM-CSF, CCL17 and CCL22 in the airway wall (**Supplementary Fig. 2**) as compared to allergic mice treated with a nonsense siRNA. Conversely, treatment of naive mice with rTRAIL increased IL-25 and IL-33 expression (**Fig. 1h**), which suggests that these factors are regulated by MID1 downstream of TRAIL. MID1 silencing also increased PP2A activity (**Fig. 1i**) and reduced the levels of phosphorylated IκBα, the NF-κB

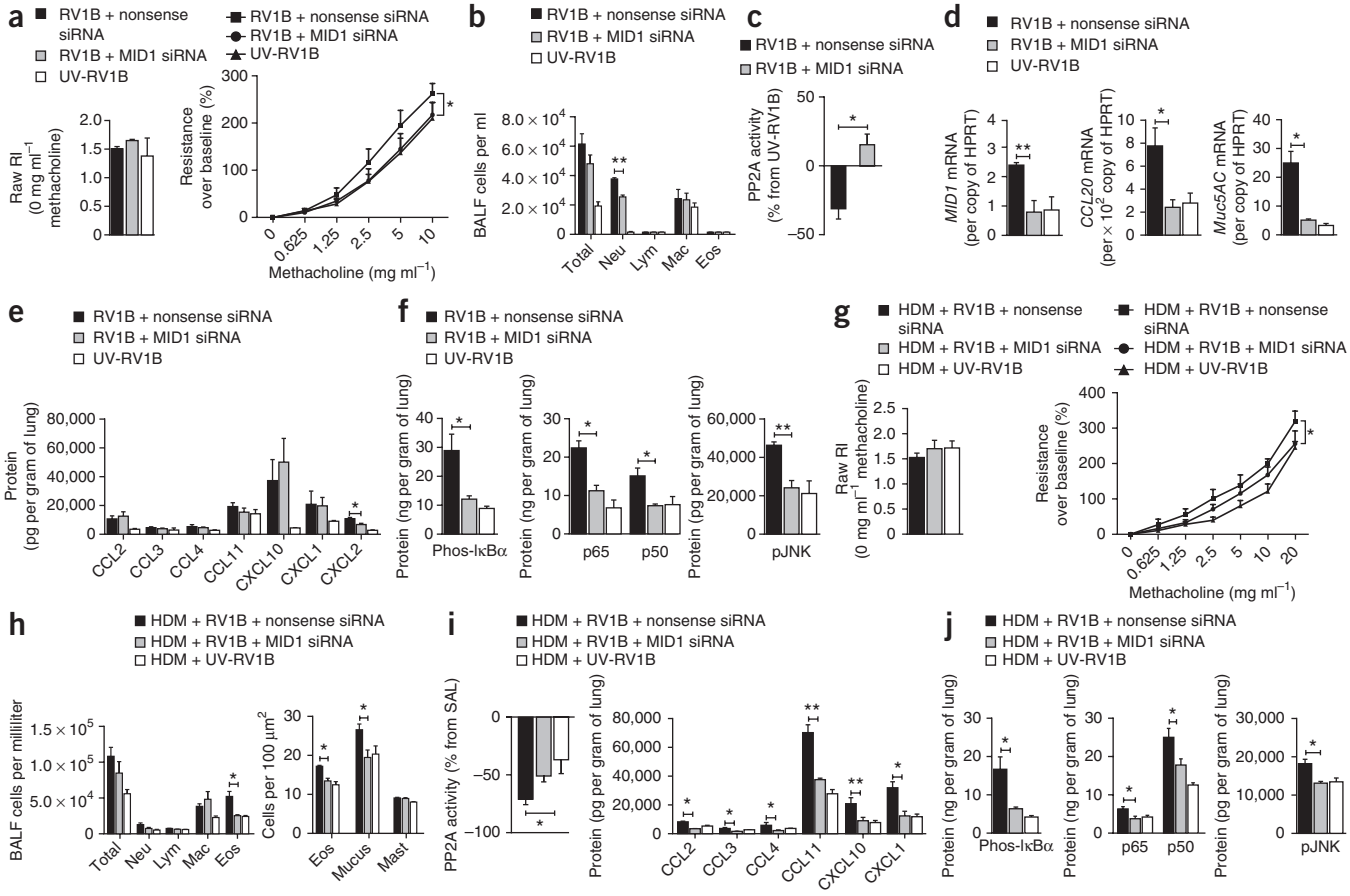

Figure 3 MID1 inhibition attenuates rhinovirus-induced airway inflammation and asthma exacerbations. (**a**) Total lung resistance (RI) at baseline (left) and as percentage change of baseline measurement (PBS) in response to inhaled methacholine (right) in mice treated with nonsense siRNA or MID1 siRNA 24 h before intranasal RV1B (n = 5 or 6 mice per group). (**b**) Number of cells in the BALF of mice in **a**. (**c**–**f**) PP2A activity in lung homogenates (**c**), *MID1*, *CCL20* and mucin 5AC (*muc5AC*) mRNA expression in the airway wall (**d**), chemokine levels (**e**) and phosphorylated IκBα (left), p65, p50 (middle) and phosphorylated JNK (pJNK; right) protein levels (**f**) in lung homogenates of mice from **a** (n = 3 or 4 mice per group). (**g**) Total lung resistance at baseline (left) and as percentage change of baseline measurement (PBS) in response to inhaled methacholine (right) in the airways of HDM-allergic mice treated with nonsense siRNA or MID1 siRNA 24 h before intranasal infection with RV1B (n = 6–8 mice per group). (**h**) Number of cells in BALF (left) and number of peribronchial/perivascular eosinophils, PAS-positive mucus producing epithelial cells, and mast cells per 100 μm² (right) in the lungs of mice from **g**. (**i**,**j**) PP2A activity (left), chemokine amounts (**i**) and phosphorylated IκBα (left), p65, p50 (middle) and phosphorylated JNK (right) protein levels in lung homogenates of mice from **g** (**j**). Results are mean ± s.e.m. (n = 3–6 mice per group). *P < 0.05 and **P < 0.01.

© 2013 Nature America, Inc. All rights reserved.

subunits p65, p50, p52 and RelB (**Fig. 1i**), and phosphorylated JNK in lung homogenates (**Fig. 1j**), and phosphorylated p38 MAPK measured by quantification of immunofluorescence (**Fig. 1j** and **Supplementary Fig. 3**). Similar results with respect to AHR, airway inflammation and PP2A activity were obtained when silencing MID1 using another MID1-specific siRNA sequence (**Supplementary Fig. 4**). Thus MID1 expression promotes allergic airway disease and limits PP2A-mediated deactivation of NF-κB, p38 MAPK and JNK.

Next, we treated sensitized mice 24 h before the first challenge with HDM and then daily with the nonphosphorylatable FTY720 analog, 2-amino-4-(4-heptyloyphenol)-2-methylbutanol ($AAL_{(S)}$) to activate PP2A (**Fig. 2a**). In contrast to phosphorylated FTY720, $AAL_{(S)}$ does not cause lymphopenia because it cannot be phosphorylated by sphingosine kinase 2 and bind sphingosine 1-phosphate receptors (ref. 36 and **Fig. 2b**). $AAL_{(S)}$ treatment increased PP2A activation, decreased MID1 expression (**Fig. 2c**) and reduced allergic airway disease, which included decreased AHR (**Fig. 2d**), inflammatory cell recruitment to the lung (**Fig. 2e**,**f**), release of IL-5 and IL-13 by lymph node cells (**Fig. 2g**), and decreased expression of CCL20, IL-25 and IL-33 (**Fig. 2h**) but not TSLP, GM-CSF, CCL17 and CCL22 in the airway wall (**Supplementary Fig. 5**). The effects of $AAL_{(S)}$ on MID1 expression may indicate feedback inhibition by the adaptor protein α4 (ref. 23) or could be due to the anti-inflammatory effects of $AAL_{(S)}$. We and others have previously shown a link between CCL20 and the activation of T cells in an ovalbumin-induced allergic airway disease model[4,37]. In accordance with this link, we observed a significant decrease in T cell numbers and in the ratio of myeloid to plasmacytoid dendritic cells in the lungs of $AAL_{(S)}$-treated mice (**Fig. 2i**), which suppresses the development of T_H2-mediated responses *in vivo*[3,38]. These data suggest that pharmacological activation of PP2A may be therapeutically effective in allergic airway disease and asthma.

Next, we investigated the role of MID1 in experimental rhinovirus infection. First we silenced MID1 expression in naive mice using siRNA 24 h before infecting mice with rhinovirus (RV1B) (or ultraviolet light–inactivated RV1B). Silencing of MID1 abolished RV1B-induced AHR, reduced neutrophil influx, increased PP2A activity, decreased MID1, CCL20, mucin 5AC (a major gel-forming mucin expressed in the airways[39]) and CXCL2 (a mouse IL-8 analog)

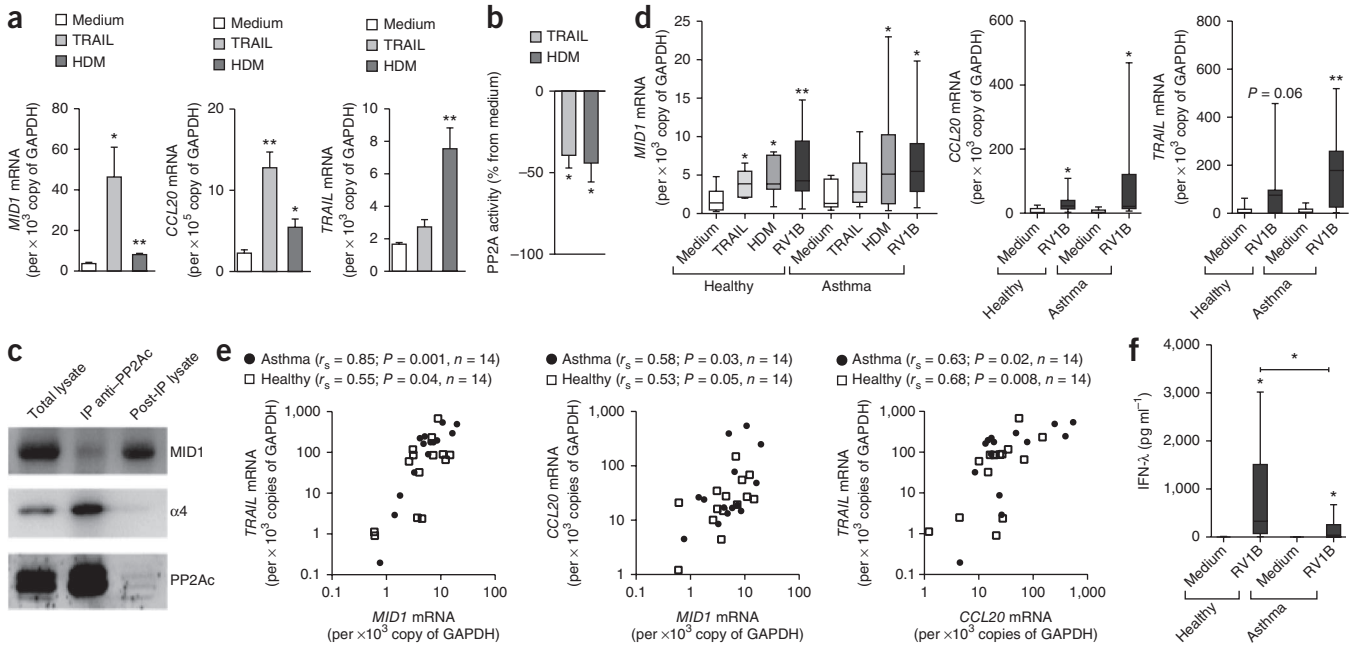

Figure 4 MID1 in allergen and rhinovirus exposed human airway epithelial cells. (**a**,**b**) *MID1*, *CCL20* and *TRAIL* mRNA expression (**a**) and PP2A activity (**b**) in BEAS-2B cells incubated with HDM extract (50 μg ml^{-1}), or recombinant TRAIL (1 μg ml^{-1}). Results are representative of $n = 3$ independent experiments. (**c**) Immunoprecipitation (IP) for PP2Ac in unstimulated BEAS-2B cell lysates. Total lysate (lane 1), PP2Ac precipitant (lane 2), PP2Ac-depleted lysate (lane 3). (**d**) *MID1* expression (left) in primary bronchial epithelial cells from healthy subjects and asthmatics incubated with control medium, HDM extract (50 μg ml^{-1}), rTRAIL (1 μg ml^{-1}), or infected with RV1B. *CCL20* (middle) and *TRAIL* (right) expression in bronchial epithelial cells in response to RV1B infection. Lines indicate the median, boxes extend from the 25th to the 75th percentile and error bars extend to 10th and 90th percentiles. (**e**) Correlation between *MID1*, *TRAIL* and *CCL20* mRNA expression in primary human airway epithelial cells after RV1B infection ($n = 14$ asthmatics and $n = 14$ healthy subjects). (**f**) IFN-λ concentration in primary bronchial epithelial cell supernatants from healthy subjects and subjects with asthma after infection with RV1B. Lines indicate the median, boxes extend from the 25th to the 75th percentile and error bars extend to the 10th and 90th percentiles.* $P < 0.05$ and ** $P < 0.01$.

© 2013 Nature America, Inc. All rights reserved.

expression in the lungs, and reduced the amounts of phosphorylated IκBα, activated NF-κB subunits and phosphorylated JNK compared to nonsense siRNA treatment (**Fig. 3a–f**). MID1 inhibition also impaired virus replication and, consequently, interferon-α (IFN-α) and IFN-β mRNA expression in the lung of RV1B-infected mice (**Supplementary Fig. 6**). Next, we silenced MID1 expression in allergic mice with one dose of siRNA given after the last HDM challenge and then infected them with RV1B 24 h later. MID1 silencing reduced rhinovirus-induced exacerbation of AHR, eosinophilic inflammation and the number of mucus-producing epithelial cells (**Fig. 3g**,**h**). MID1 inhibition also raised PP2A activity, impaired chemokine release and lowered levels of phosphorylated IκBα, activated NF-κB subunits and phosphorylated JNK in the lung of RV1B-infected allergic mice (**Fig. 3i**,**j**). After *ex vivo* recall stimulation of peribronchial lymph node cells isolated from RV1B-infected allergic mice with HDM, production of IL-5 (nonsense siRNA, 8.6 ± 0.6 ng ml^{-1} versus MID1-siRNA 3.2 ± 0.6 ng ml^{-1}; mean ± s.e.m., $P < 0.01$) but not IL-13 (data not shown) was reduced. Virus replication and IFN expression in the airway wall was not altered in allergic mice in response to MID1 inhibition (**Supplementary Fig. 6**).

Next, we incubated transformed human bronchial epithelial cells (BEAS-2B) with rTRAIL or HDM and found they increased MID1 and CCL20 mRNA expression (**Fig. 4a**) and suppressed PP2A activity (**Fig. 4b**). Western blotting and immunoprecipitation with a PP2Ac-specific antibody suggested that MID1 was associated with PP2Ac and the α4 subunit (**Fig. 4c**).

Differences between transformed and primary human epithelial cell responses to rhinovirus have been described[40]. We therefore also collected primary human bronchial epithelial cells from subjects with asthma ($n = 14$) and healthy subjects ($n = 14$). As expected, lung function was lower in individuals with asthma ($P < 0.05$), and the majority of those subjects were treated with inhaled corticosteroids (**Supplementary Table 1**). *In vitro* infection with RV1B as well as exposure to rTRAIL or HDM increased MID1 expression in epithelial cells from both healthy subjects and those with asthma (**Fig. 4d**). TRAIL and CCL20 expression were also upregulated upon RV1B infection (**Fig. 4d**) and positively correlated with MID1 expression (**Fig. 4e**). We found impaired IFN-λ production by bronchial epithelial cells from asthmatics as compared to cells from healthy subjects as previously reported[12,13] (**Fig. 4f**). Intracellular RV1B RNA levels isolated from epithelial cells 24 h after infection were not different between asthmatics and healthy subjects (**Supplementary Fig. 6**), which is in line with previous reports demonstrating *in vitro* differences in RV1B RNA levels at 8 h only when virus replication peaks[12,13]. Thus, MID1 activates proinflammatory signaling in bronchial epithelial cells from human subjects, which may act in concert with other aberrant responses to allergen and virus exposure in asthma to promote exaggerated airway inflammation and rhinovirus-induced exacerbation.

More than 500 E3 ubiquitin ligases have been identified to date that regulate diverse cellular processes through targeting specific substrates for degradation by the proteasome. The ubiquitin system has been linked to cancer, neurodegenerative and muscle wasting disorders, diabetes, infection and inflammation. Here we have identified MID1 as an E3 ubiquitin ligase that regulates airway inflammation by limiting PP2A activity (**Supplementary Fig. 7**) suggesting both MID1

and PP2A activity may be targeted for the treatment of asthma and rhinovirus-induced exacerbations.

METHODS

Methods and any associated references are available in the online version of the paper.

Note: Supplementary information is available in the online version of the paper.

ACKNOWLEDGMENTS

This study was supported by the National Health and Medical Research Council (NH&MRC 631075 and 1011153) (J.M., P.S.F., N.V.), the Hunter Medical Research Institute (J.M., P.A.B.W., P.S.F.), the Hunter Children's Research Foundation (J.M., P.S.F., A.P.d.S.) and an NH&MRC Health Practitioner Research Fellowship to J.M. (455623). N.W.B. was supported by a project grant from Asthma UK (06-050) and S.L.J. by a Chair from Asthma UK (CH1155). This work was supported in part by MRC Centre grant G1000758 and ERC FP7 Advanced grant 233015 (to S.L.J.). We would like to thank M. Smyth, Peter MacCallum Cancer Centre, and J. Peschon, Amgen, for providing *Tnfsf10*$^{-/-}$ mice and S. Akira, Osaka University, for providing *Tlr4*$^{-/-}$ and *Myd88*$^{-/-}$ mice. We appreciate technical assistance from C. Cesar de Souza Alves, F. Eyers, J. Girkin, J. Grehan, H. MacDonald, M. Morten, K. Parsons, S. Reeves, L. Sokulsky and the staff from the animal care facilities of the contributing institutes.

AUTHOR CONTRIBUTIONS

A.C. and L.H. performed and designed mouse and cell culture experiments, analyzed data, generated figures and edited the manuscript. P.A.B.W. and M.T. performed and supervised studies on healthy subjects and subjects with asthma and performed cell culture experiments. N.V. and H.C. performed and analyzed PP2Ac measurements and immunoprecipitation and designed experiments. N.V. edited the manuscript. A.S.D. and J.C.M. synthesized $AAL_{(S)}$ for use as an activator of PP2A and developed the dosing regiment. N.Z. and M.E.R. coordinated and assisted in microarray array analysis. N.W.B. and S.L.J. assisted in design of experiments, provided RV1B for further propagation and cDNAs and edited the manuscript. A.P.d.S. coordinated and supervised mouse and human studies. P.S.F. supervised mouse studies, interpreted data and edited the manuscript. J.M. conceptualized, coordinated, designed and supervised mouse and human studies, interpreted and analyzed data, and drafted and edited the manuscript. All authors contributed to data discussion and revised the manuscript.

COMPETING FINANCIAL INTERESTS

The authors declare competing financial interests: details are available in the online version of the paper.

Published online at http://www.nature.com/doifinder/10.1038/nm.3049.
Reprints and permissions information is available online at http://www.nature.com/reprints/index.html.

© 2013 Nature America, Inc. All rights reserved.

1. Lemanske, R.F. Jr. & Busse, W.W. Asthma: clinical expression and molecular mechanisms. *J. Allergy Clin. Immunol.* **125**, S95–S102 (2010).
2. Holgate, S.T., Roberts, G., Arshad, H.S., Howarth, P.H. & Davies, D.E. The role of the airway epithelium and its interaction with environmental factors in asthma pathogenesis. *Proc. Am. Thorac. Soc.* **6**, 655–659 (2009).
3. Lambrecht, B.N. & Hammad, H. Biology of lung dendritic cells at the origin of asthma. *Immunity* **31**, 412–424 (2009).
4. Weckmann, M. *et al.* Critical link between TRAIL and CCL20 for the activation of TH2 cells and the expression of allergic airway disease. *Nat. Med.* **13**, 1308–1315 (2007).
5. Wills-Karp, M. *et al.* Interleukin-13: central mediator of allergic asthma. *Science* **282**, 2258–2261 (1998).
6. Kuperman, D.A. *et al.* Direct effects of interleukin-13 on epithelial cells cause airway hyperreactivity and mucus overproduction in asthma. *Nat. Med.* **8**, 885–889 (2002).
7. Mattes, J. *et al.* IL-13 induces airways hyperreactivity independently of the IL-4R alpha chain in the allergic lung. *J. Immunol.* **167**, 1683–1692 (2001).
8. Kuperman, D., Schofield, B., Wills-Karp, M. & Grusby, M.J. Signal transducer and activator of transcription factor 6 (Stat6)-deficient mice are protected from antigen-induced airway hyperresponsiveness and mucus production. *J. Exp. Med.* **187**, 939–948 (1998).
9. Johnston, S.L. *et al.* Community study of role of viral infections in exacerbations of asthma in 9–11 year old children. *Br. Med. J.* **310**, 1225–1229 (1995).
10. Kusel, M.M. *et al.* Role of respiratory viruses in acute upper and lower respiratory tract illness in the first year of life: a birth cohort study. *Pediatr. Infect. Dis. J.* **25**, 680–686 (2006).
11. Jackson, D.J. *et al.* Wheezing rhinovirus illnesses in early life predict asthma development in high-risk children. *Am. J. Respir. Crit. Care Med.* **178**, 667–672 (2008).
12. Wark, P.A. *et al.* Asthmatic bronchial epithelial cells have a deficient innate immune response to infection with rhinovirus. *J. Exp. Med.* **201**, 937–947 (2005).
13. Contoli, M. *et al.* Role of deficient type III interferon-λ production in asthma exacerbations. *Nat. Med.* **12**, 1023–1026 (2006).
14. Holgate, S.T. A look at the pathogenesis of asthma: the need for a change in direction. *Discov. Med.* **9**, 439–447 (2010).
15. Crimi, E. *et al.* Dissociation between airway inflammation and airway hyperresponsiveness in allergic asthma. *Am. J. Respir. Crit. Care Med.* **157**, 4–9 (1998).
16. Phipps, S. *et al.* Toll/IL-1 signaling is critical for house dust mite-specific T_H1 and T_H2 responses. *Am. J. Respir. Crit. Care Med.* **179**, 883–893 (2009).
17. Hammad, H. *et al.* House dust mite allergen induces asthma via Toll-like receptor 4 triggering of airway structural cells. *Nat. Med.* **15**, 410–416 (2009).
18. Mattes, J., Collison, A., Plank, M., Phipps, S. & Foster, P.S. Antagonism of microRNA-126 suppresses the effector function of T_H2 cells and the development of allergic airways disease. *Proc. Natl. Acad. Sci. USA* **106**, 18704–18709 (2009).
19. Kumar, H., Kawai, T. & Akira, S. Toll-like receptors and innate immunity. *Biochem. Biophys. Res. Commun.* **388**, 621–625 (2009).
20. Fontanella, B., Russolillo, G. & Meroni, G. MID1 mutations in patients with X-linked Opitz G/BBB syndrome. *Hum. Mutat.* **29**, 584–594 (2008).
21. Latta, E.J. & Golding, J.P. Regulation of PP2A activity by Mid1 controls cranial neural crest speed and gangliogenesis. *Mech Dev.* **128**, 560–576 (2012).
22. Aranda-Orgillés, B. *et al.* Active transport of the ubiquitin ligase MID1 along the microtubules is regulated by protein phosphatase 2A. *PLoS ONE* **3**, e3507 (2008).
23. McConnell, J.L. *et al.* α4 is a ubiquitin-binding protein that regulates protein serine/threonine phosphatase 2A ubiquitination. *Biochemistry* **49**, 1713–1718 (2010).
24. Trockenbacher, A., Suckow, V., Foerster, J., Winter, J. & Krauss, S. MID1, mutation in Opitz syndrome, encodes an ubiquitin ligase that targets phophatase 2A for degradation. *Nat. Genet.* **29**, 287–294 (2001).
25. Watkins, G.R. *et al.* Monoubiquitination promotes calpain cleavage of the protein phosphatase 2A (PP2A) regulatory subunit α4, altering PP2A stability and microtubule-associated protein phosphorylation. *J. Biol. Chem.* **287**, 24207–24215 (2012).
26. Sim, A.T., Ludowyke, R.I. & Verrills, N.M. Mast cell function: regulation of degranulation by serine/threonine phosphatases. *Pharmacol. Ther.* **112**, 425–439 (2006).
27. Cornell, T.T. *et al.* Ceramide-dependent PP2A regulation of TNFα-induced IL-8 production in respiratory epithelial cells. *Am. J. Physiol. Lung Cell Mol. Physiol.* **296**, L849–L856 (2009).
28. Shanley, T.P., Vasi, N., Denenberg, A. & Wong, H.R. The serine/threonine phosphatase, PP2A: endogenous regulator of inflammatory cell signaling. *J. Immunol.* **166**, 966–972 (2001).
29. Miskolci, V. *et al.* Okadaic acid induces sustained activation of NFκB and degradation of the nuclear IκBα in human neutrophils. *Arch. Biochem. Biophys.* **417**, 44–52 (2003).
30. Liu, W. *et al.* Cell-specific activation profile of extracellular signal-regulated kinase 1/2, Jun N-terminal kinase, and p38 mitogen-activated protein kinases in asthmatic airways. *J. Allergy Clin. Immunol.* **121**, 893–902.e2 (2008).
31. Griego, S.D., Weston, C.B., Adams, J.L., Tal-Singer, R. & Dillon, S.B. Role of p38 mitogen-activated protein kinase in rhinovirus-induced cytokine production by bronchial epithelial cells. *J. Immunol.* **165**, 5211–5220 (2000).
32. Duan, W. *et al.* Inhaled p38α mitogen-activated protein kinase antisense oligonucleotide attenuates asthma in mice. *Am. J. Respir. Crit. Care Med.* **171**, 571–578 (2005).
33. Wong, W.S. Inhibitors of the tyrosine kinase signaling cascade for asthma. *Curr. Opin. Pharmacol.* **5**, 264–271 (2005).
34. Das, J. *et al.* A critical role for NF-κB in GATA3 expression and T_H2 differentiation in allergic airway inflammation. *Nat. Immunol.* **2**, 45–50 (2001).
35. Kobayashi, Y., Mercado, N., Barnes, P.J. & Ito, K. Defects of protein phosphatase 2a causes corticosteroid insensitivity in severe asthma. *PLoS ONE* **6**, e27627 (2011).
36. Don, A.S. *et al.* Essential requirement for sphingosine kinase 2 in a sphingolipid apoptosis pathway activated by FTY720 analogues. *J. Biol. Chem.* **282**, 15833–15842 (2007).
37. Francis, J.N., Sabroe, I., Lloyd, C.M., Durham, S.R. & Till, S.J. Elevated $CCR6^+$ $CD4^+$ T lymphocytes in tissue compared with blood and induction of CCL20 during the asthmatic late response. *Clin. Exp. Immunol.* **152**, 440–447 (2008).
38. Lambrecht, B.N. *et al.* Myeloid dendritic cells induce T_H2 responses to inhaled antigen, leading to eosinophilic airway inflammation. *J. Clin. Invest.* **106**, 551–559 (2000).
39. Ehrle, C. *et al.* Overexpressing mouse model demonstrates the protective role of Muc5ac in the lungs. *Proc. Natl. Acad. Sci. USA.* **109**, 16528–16533 (2012).
40. Xatzipsalti, M. & Papadopoulos, N.G. Cellular and animals models for rhinovirus infection in asthma. *Contrib. Microbiol.* **14**, 33–41 (2007).

ONLINE METHODS

Mice. WT, *Tnfsf10*$^{-/-}$, *Tlr4*$^{-/-}$, *Myd88*$^{-/-}$and *Stat6*$^{-/-}$, all on a BALB/c background (male, 6–14 weeks of age) were obtained from the special pathogen–free facility of the University of Newcastle. Mice were housed with *ad libitum* access to food and water with a 12-h light-and-dark cycle. The Animal Care and Ethics Committee of the University of Newcastle, Australia approved all experiments, which were conducted and reported in accordance with the ARRIVE guidelines.

Induction of allergic airway disease and rhinovirus infection. We sensitized and challenged mice by exposing them intranasally to crude HDM extract (50 μg daily at days 0, 1 and 2 followed by four exposures of 5 μg HDM daily from day 14 to day 17 delivered in 50 μl of sterile saline) from Greer Laboratories (allergic mice). The single dose of HDM extract given to naive mice in some experiments was 50 μg in 50 μl of sterile saline. Control nonallergic mice received sterile saline only during sensitization and challenge instead of HDM extract. In some experiments, we infected allergic (day 18, 1 d after last HDM extract challenge) or nonallergic mice with 50 μl infective or ultraviolet light (UV)–inactivated RV1B[41] (2.5×10^6 median tissue culture infective dose) intranasally. Mice were killed 24 h after the last allergen or rhinovirus challenge by pentobarbital sodium (Virbac) overdose.

Airway hyperreacticity measurement (AHR). We assessed AHR invasively in separate groups of ketamine-xylene (Illum)–anesthetized mice by measurement of total lung resistance and dynamic compliance (Buxco)[4]. Percentage increase over baseline (PBS) in response to nebulized methacholine (Sigma) was calculated.

Isolation of mRNA. We isolated total RNA with the mirVana m/miRNA Isolation kit (Ambion) from mouse airway wall tissue[18]. Briefly, we isolated the trachea and lungs and then carefully separated the lung parenchyma from the larger airway tissue by blunt dissection using two pairs of forceps. This allowed effective collection of several generations of airway wall tissue, consisting of resident airway cells such as epithelial cells, fibroblasts, smooth muscle cells, basement membrane and infiltrating inflammatory cells[42]. Airway wall tissue was stored in RNA later (Ambion) at −80 °C before extraction. Total RNA from human bronchial epithelial cells was extracted with TRIzol (Invitrogen) according to the manufacturer's instructions.

Quantitative RT-PCR. We performed quantitative RT-PCRs with SYBR Green with premixed ROX (Invitrogen). We quantified mRNA copies using cDNA standards for all genes of interest. We normalized expression to the housekeeper genes *Hprt* for mouse and *GAPDH* for human mRNAs. Primers are listed in the **Supplementary Methods**.

Airway inflammation. We cannulated the trachea of mice and lavaged their lungs with 1 ml HBSS (Gibco) to collect bronchoalveolar cells, which were enumerated and differentiated by cytospin and May-Grunwald staining under blinded conditions.

Airway morphology studies. We stained paraffin-fixed lung tissue with Alcian blue–periodic acid–Schiff for the enumeration of mucus-producing airway epithelial cells, Charbol's chromotrope-hematoxylin for the identification of eosinophils or toluidine blue for mast cells. We identified cells by morphological criteria, and we counted ten 100-μm^2 fields in each slide under blinded conditions.

Cytokine and chemokine analysis. We excised peribronchial lymph node cells, filtered through a 100-μm cell sieve (BD) and cultured 5×10^6 cells per ml in RPMI-1640 medium (Hyclone) with 10% (vol/vol) FCS (SAFC Biosciences), 2 mM L-glutamine, 20 mM HEPES, 100 U ml^{-1} penicillin-streptomycin (Gibco), 0.1 mM sodium pyruvate (Hyclone) and 50 μM 2-mercaptoethanol in the presence or absence of 50 μg ml^{-1} HDM (optimal concentration) for 6 d. We determined IL-4, IL-5, IL-13 and IFN-γ levels in supernatants by ELISA (BD Biosciences Pharmingen). Lungs were homogenized using a Tissue-Tearor stick homogenizer (BioSpec Products). Homogenate levels of CCL2/MCP1, CCL3/MIP1α, CCL4/MIP1β, CCL11/eotaxin, CXCL10/IP10 and CXCL1/KC were measured by employing a Multiplex Immunoassay (Millipore), whereas CCL20/MIP3α and CXCL2/MIP2 were measured by ELISA (R&D Systems) according to the manufacturer's instructions.

Total PP2Ac ELISA and active PP2A, IκBα, NFκB and JNK assays. We measured total PP2Ac and PP2A activity and phosphorylated JNK by R&D Systems' Total PP2Ac DuoSet IC ELISA kit, Active PP2A DuoSet IC activity assay and Phospho-JNK DuoSet IC ELISA kit, respectively, according to the manufacturer's instructions. We quantified phosphorylated IκBα and activated p50, p52, p65 and RelB NF-κB subunits with FunctionalELISA and TransAM Transcription Factor Assay kit from Active Motif, respectively, according to the manufacturer's instructions. All measurements were performed on homogenized mouse lungs using a Tissue-Tearor stick homogenizer (BioSpec Products) or clarified BEAS-2B cell lysates (cell line obtained from ATCC).

siRNA. The antisense strand sequence of siRNA-MID1 from Ambion was: 5′-UUAGGUAAUCCAGACAUUCta-3′. A second siRNA-MID1 was ordered from Dharmacon to evaluate off-target effects (target sequence 5′-UGAGCGCUAUGACAAAUUG-3′). We ordered the two nonsense siRNA (chosen to have an equivalent CG content) with no similarities to other sequences from Ambion (Option 2) and Dharmacon. We administered 3.75 nmol siRNA in 25 μl of sterile saline intranasally at day 13 (after HDM sensitization and 24 h before first HDM challenge) and then every second day until mice were killed[4]. In all rhinovirus studies, mice were treated 24 h before and killed 24 h after RV1B challenge.

$AAL_{(S)}$ treatment. We treated mice with 10 μg of $AAL_{(S)}$ or 2% 2-hydroxypropyl-cyclodextrin (vehicle) intranasally at day 13 (after HDM sensitization and 24 h before the first HDM challenge) and then daily throughout the HDM challenge period until mice were killed.

Immunofluorescent detection. Formalin-fixed lung sections were blocked with 25% (vol/vol) sheep serum (SAFC Biosciences) for 1 h before being incubated with either an MID1-specific antibody (Santa Cruz Biotechnology, cat. no. sc-55247, 1:200) followed by a secondary PE-conjugated antibody (Santa Cruz Biotechnology, cat no. sc-3743, clone 2BB10, 1:2,000), or an Alexa Fluor 488–conjugated antibody against phosphorylated p38 (Cell Signaling Technology, cat. no. 4551S, clone 28B10, 1:200). Nuclei were counterstained with DAPI (Sigma). We analyzed stained slides with an Olympus BX51 UV microscope using DP Controller 3.1.1.267 software (Olympus). Fluorescent intensity was quantified using Image-ProPlus 6.0 software, measuring red channel (phycoerythrin-stained MID-1) or green channel (Alexa Fluor 488–stained Phos-p38) intensity in the airway epithelial cells of ten high-powered fields per slide under blinded conditions.

Immunoprecipitation. We lysed BEAS-2B cells at 80% confluency in the presence of protease inhibitors (pepstatin, leupeptin, aprotinin and PMSF; Sigma). Protein lysate (500 mg) was incubated with 4 mg PP2A-C monoclonal antibody (clone 1D6, 1:5,000, Millipore) and protein A agarose beads (Millipore) at 4 °C overnight followed by three washes in lysis buffer. We separated immunoprecipitated proteins on 12% (wt/vol) polyacryamide gels and transferred them to nitrocellulose. We probed immunoblots with primary polyclonal antibodies to PP2Ac (affinity-purified rabbit antibodies raised against a PP2Ac peptide (PHVTRRTPDYFL), 1:1,000)[43], α4 (Novus Biologicals, cat. no. NB100-487, 1:500) or MID1 (Santa Cruz Biotechnology, cat. no. sc-55248, 1:200) and appropriate secondary antibodies as described above.

Flow cytometry. We dissociated mouse lung cells mechanically and stained whole lung cell suspensions with FITC-conjugated anti–TCR β chain (BD, cat. no. 553171, clone H57-597), phycoerythrin-conjugated anti-CD4 (BD, cat. no. 553652, clone H129.19), PerCP-conjugated anti-CD8a (BD, cat. no. 561092, clone 53-6.7), PerCP-Cy5.5–conjugated anti-CD11b (BD, cat. no. 561092, clone M1/70), FITC-conjugated anti-CD11c (BD, cat. no. 553801, clone HL3), phycoerythrin-conjugated anti-MHCII (eBioscience, cat. no. 12-5321, clone M5/114.15.2) and allophycocyanin-conjugated anti-mPDCA-1

© 2013 Nature America, Inc. All rights reserved.

(Miltenyi Biotec, cat. no. 130-091-963, clone JF05-1C2.4.1), all at a 1:15 dilution. We determined numbers of positive cells by flow cytometry (FACSCanto, Becton Dickinson). Data were analyzed with BD FACsdiva.

Bronchial epithelium cell cultures. We cultured transformed human bronchial epithelial cells (BEAS-2B) in complete DMEM (Thermo Scientific) with 5% (vol/vol) FCS and primary human bronchial epithelial cells in bronchial epithelial cell growth medium (BEGM, Clonetics) as previously described[12]. After one passage, we seeded 2×10^5 BEAS-2B cells onto 12-well trays, cultured them until 80% confluence, serum-starved them for 24 h and incubated them with HDM (50 μg ml^{-1}) or rTRAIL (1 μg ml^{-1}) for 24 h in serum-free DMEM. Primary bronchial epithelial cells were obtained from patients with stable persistent asthma and healthy controls by bronchoscopy using a single sheathed nylon cytology brush[12]. Primary bronchial epithelial cells were seeded, cultured, and incubated under the same conditions as BEAS-2B cells with the exception of using different growth medium (BEGM). Primary bronchial epithelial cells were also infected with RV1B (multiplicity of infection of 2) and cultured for 24 h in serum-free BEGM media[12]. mRNA was extracted using TRIzol (Invitrogen) according to the manufacturer's instructions. TRAIL, MID1 and CCL20 mRNA expression were quantified by quantitative RT-PCR. We measured the concentration of IFN-λ in the cell supernatant by ELISA (IFN-λ1/3 DuoSet ELISA, R&D Systems). The Hunter New England Health and University of Newcastle Human Research Ethics Committees approved all human studies, and written informed consent was obtained from all subjects before participation.

Statistical analyses. The significance of differences between groups was analyzed using Student's *t*-test, Mann-Whitney test or two-way analysis of variance as appropriate using Graphpad Prism 5. A value of $P < 0.05$ is reported as significant. We cultured at least 13 pairs of primary bronchial epithelial cell samples per group (healthy subjects and asthmatics) in the presence or absence of RV1B to detect a significant difference in MID1 expression of 1 s.d. with a power of 90%.

41. Bartlett, N.W. *et al.* Mouse models of rhinovirus-induced disease and exacerbation of allergic airway inflammation. *Nat. Med.* **14**, 199–204 (2008).
42. Collison, A., Mattes, J., Plank, M. & Foster, P.S. Inhibition of house dust mite-induced allergic airways disease by antagonism of microRNA-145 is comparable to glucocorticoid treatment. *J. Allergy Clin. Immunol.* **128**, 160–167 (2011).
43. Sim, A.T., Collins, E., Mudge, L.M. & Rostas, J.A. Developmental regulation of protein phosphatase types 1 and 2A in post-hatch chicken brain. *Neurochem. Res.* **23**, 487–491 (1998).

© 2013 Nature America, Inc. All rights reserved.

doi:10.1038/nm.3049

The E3 ubiquitin ligase midline 1 inhibits protein phosphatase 2A activity and promotes allergen and rhinovirus-induced asthma

Adam Collison*, Luke Hatchwell*, Nicole Verrills, Peter A B Wark, Ana Pereira de Siqueira, Melinda Tooze, Helen Carpenter, Anthony S Don, Jonathan C Morris, Nives Zimmermann, Nathan W Bartlett, Marc E Rothenberg, Sebastian L Johnston, Paul S Foster & Joerg Mattes *These authors contributed equally to this work

Supplementary Fig 1

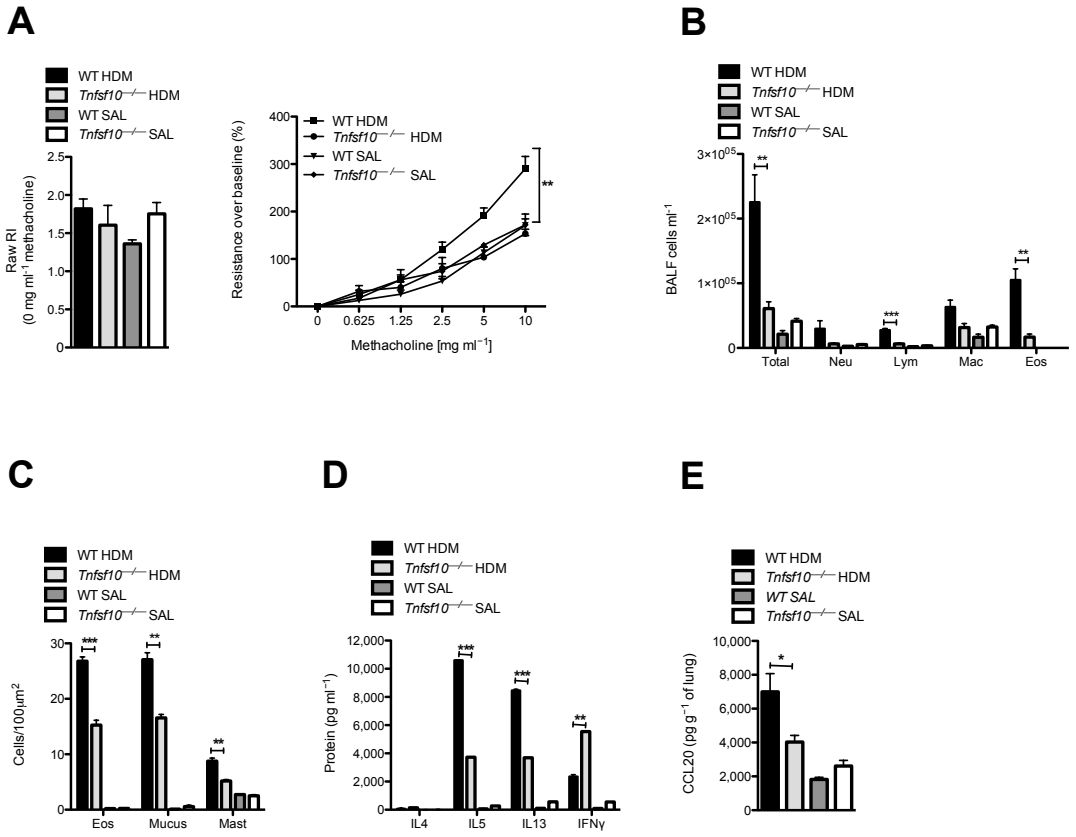

TRAIL regulates house dust mite induced allergic airways disease, MID1, and PP2A activity. (**a**) Total lung resistance (RI) as percentage change of baseline measurement (PBS) in response to inhaled methacholine in allergic (HDM) versus non-allergic (SAL) wild-type (WT) and *Tnfsf10*$^{-/-}$ mice. (n=4-12 mice per group). (**b**) Number of cells in bronchoalveolar lavage fluid (BALF) (n=3-4 mice per group). (**c**) Number of peribronchial perivacular eosinophils (x1000) and mucus-producing cells per 100μm^2. (n=3 mice per group). (**d**) Cytokine release from *in-vitro* house dust mite stimulated peribronchial lymphnode cells and (**e**) CCL20 levels in

lung homogenates. (n=4 mice per group). Results are mean±s.e.m. *, $P < 0.05$, **, $P < 0.01$, and ***, $P < 0.001$.

Supplementary Fig 2

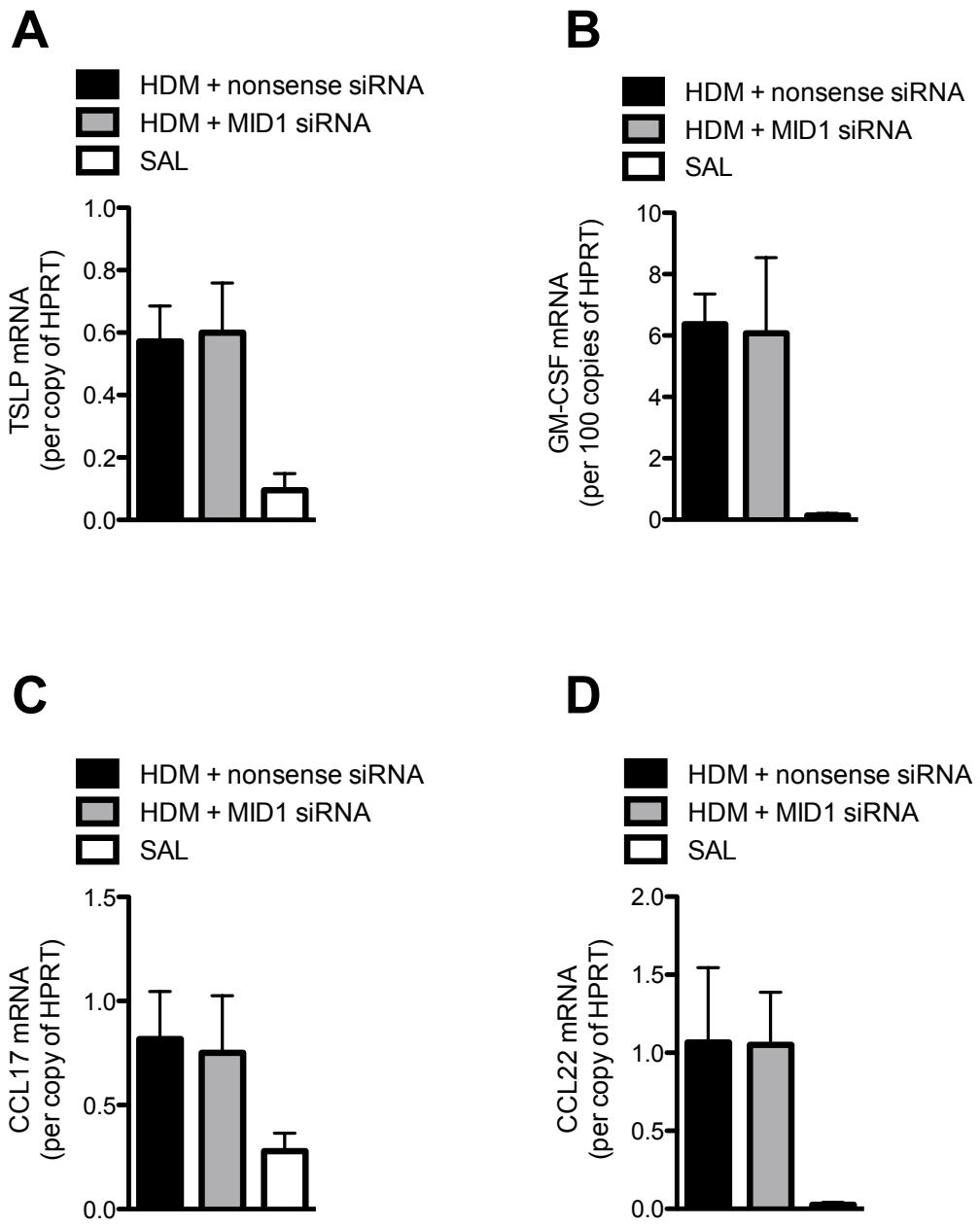

MID1 inhibition does not affect TSLP, GM-CSF, CCL17, and CCL22 RNA expression. (**a**) TSLP, (**b**) GM-CSF, (**c**) CCL17, (**d**) CCL22 mRNA expression in the airway wall of non-allergic (SAL) versus allergic (HDM) mice treated with a scrambled siRNA (nonsense siRNA) or a MID1 targeting siRNA (MID1 siRNA-2) every second day during the allergen challenge period intranasally. (n=4-6 mice per group). Results are mean±s.e.m.

Supplementary Fig 3

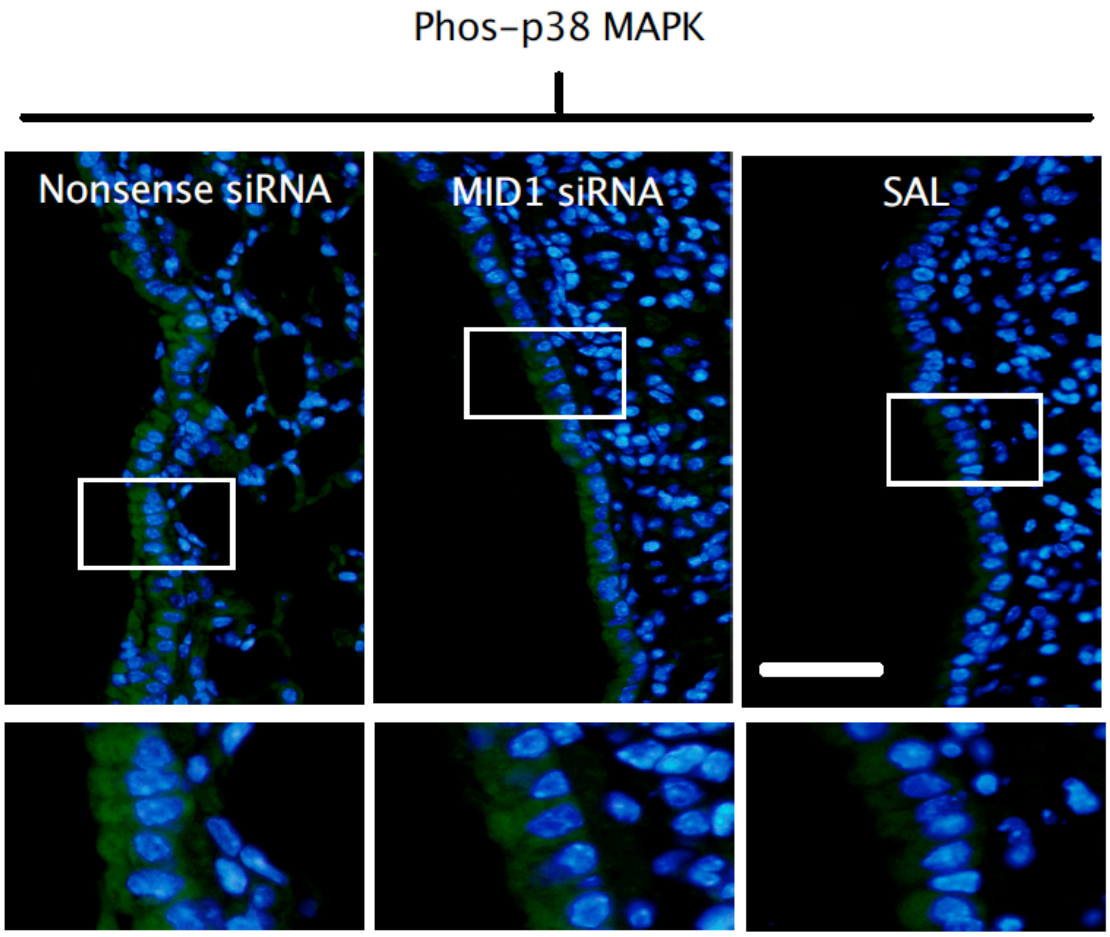

Phosphorylated p38 MAPK protein expression in the airway wall. Scale Bar, 50 µm. p38 MAPK (green); DNA (DAPI, blue).

Supplementary Fig 4

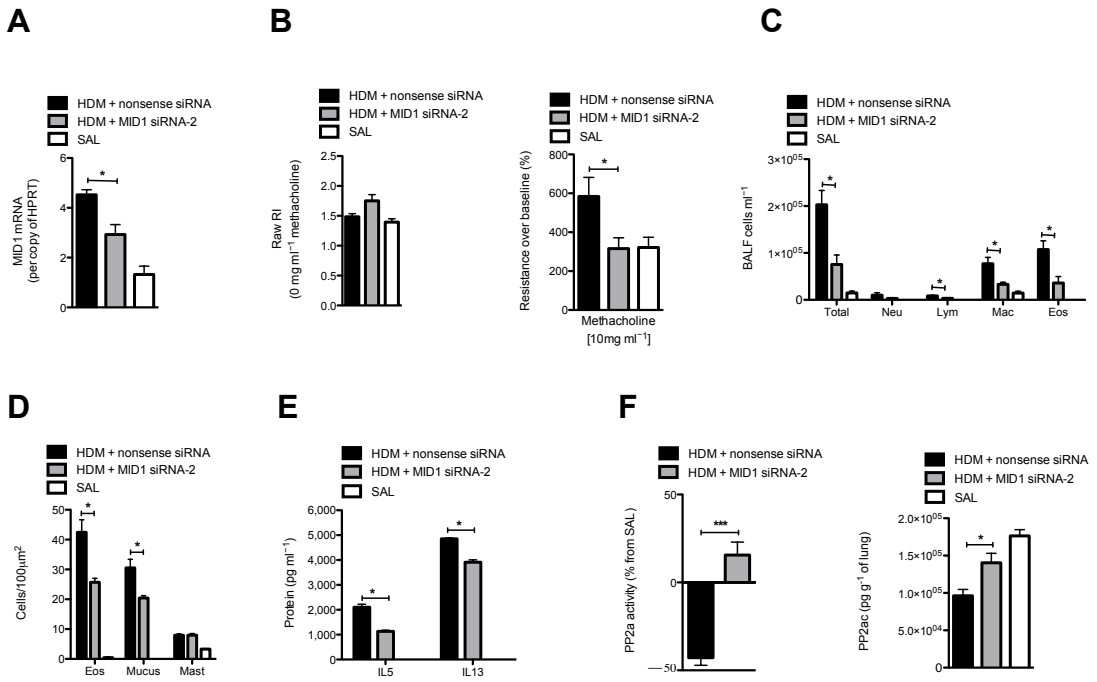

MID1 inhibition employing a different siRNA abolishes airways hyperreactivity, reduces airway inflammation and increases PP2A activity.

(**a**) MID1 mRNA in the airway wall of non-allergic (SAL) versus allergic (HDM) mice treated with a scrambled siRNA (nonsense siRNA) or a MID1 targeting siRNA (MID1 siRNA-2) every second day during the allergen challenge period intranasally. (n=3-5 mice per group). (**b**) Total lung resistance as percentage change of baseline measurement (PBS) in response to inhaled methacholine. (n=5-7 mice per group). (**c**) Number of cells in bronchoalveolar lavage fluid (BALF). (n=3 mice per group). (**d**) Number of peribronchial perivacular eosinophils, mucus-producing cells, and mast cells per 100μm^2. (n=3-4 mice per group). (**e**) Cytokine release from *in-vitro* house dust mite stimulated peribronchial lymphnode cells. (**f**) PP2A activity and PP2Ac protein concentrations in lung homogenates. (n=4 mice per group). Results are mean±s.e.m. *, $P < 0.05$ and ***, $P < 0.01$.

Supplementary Fig 5

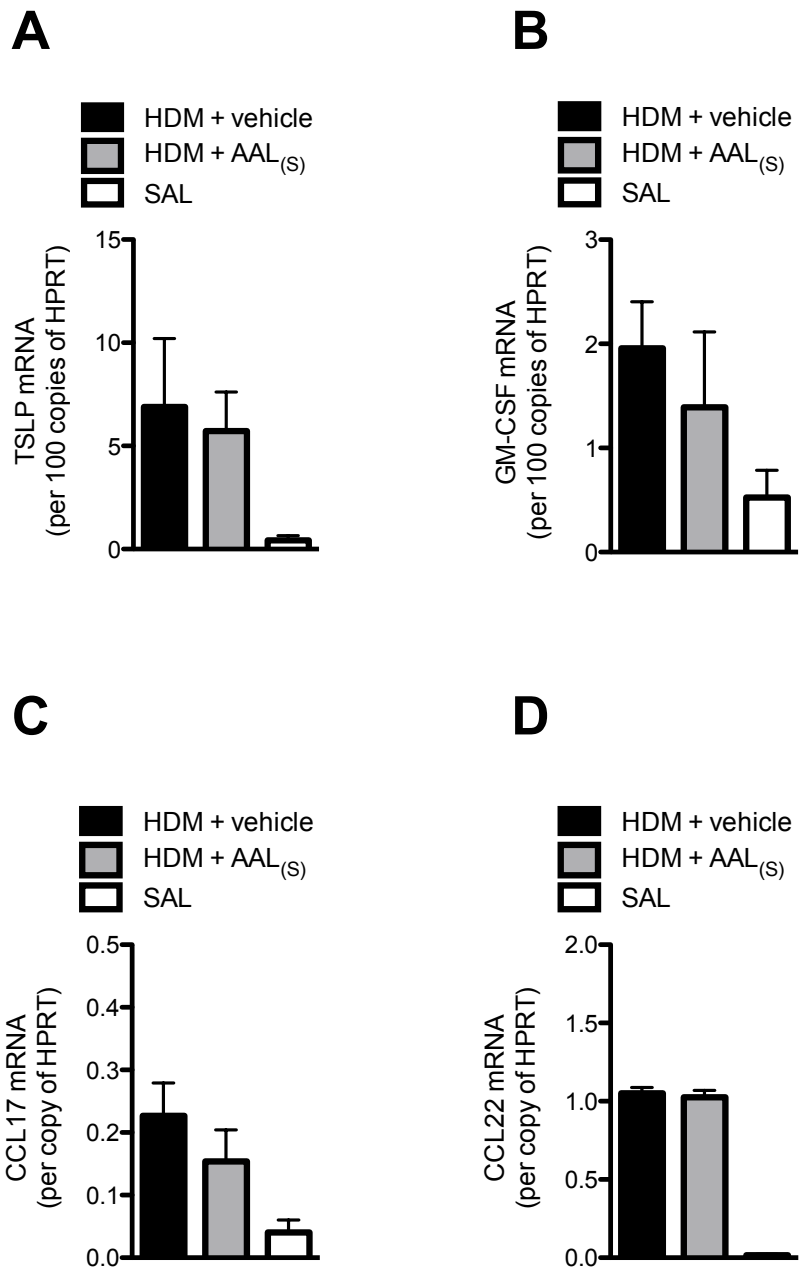

PP2A activation does not affect TSLP, GM-CSF, CCL17, and CCL22 RNA expression. (**a**) TSLP, (**b**) GM-CSF, (**c**) CCL17, (**d**) CCL22 mRNA expression in the airway wall of non-allergic (SAL) versus allergic (HDM) mice treated with 2% 2-hydroxypropyl-cyclodextrin (vehicle) or $AAL_{(S)}$ each day during the allergen challenge period intranasally. (n=3-5 mice per group). Results are mean±s.e.m.

Supplementary Fig 6

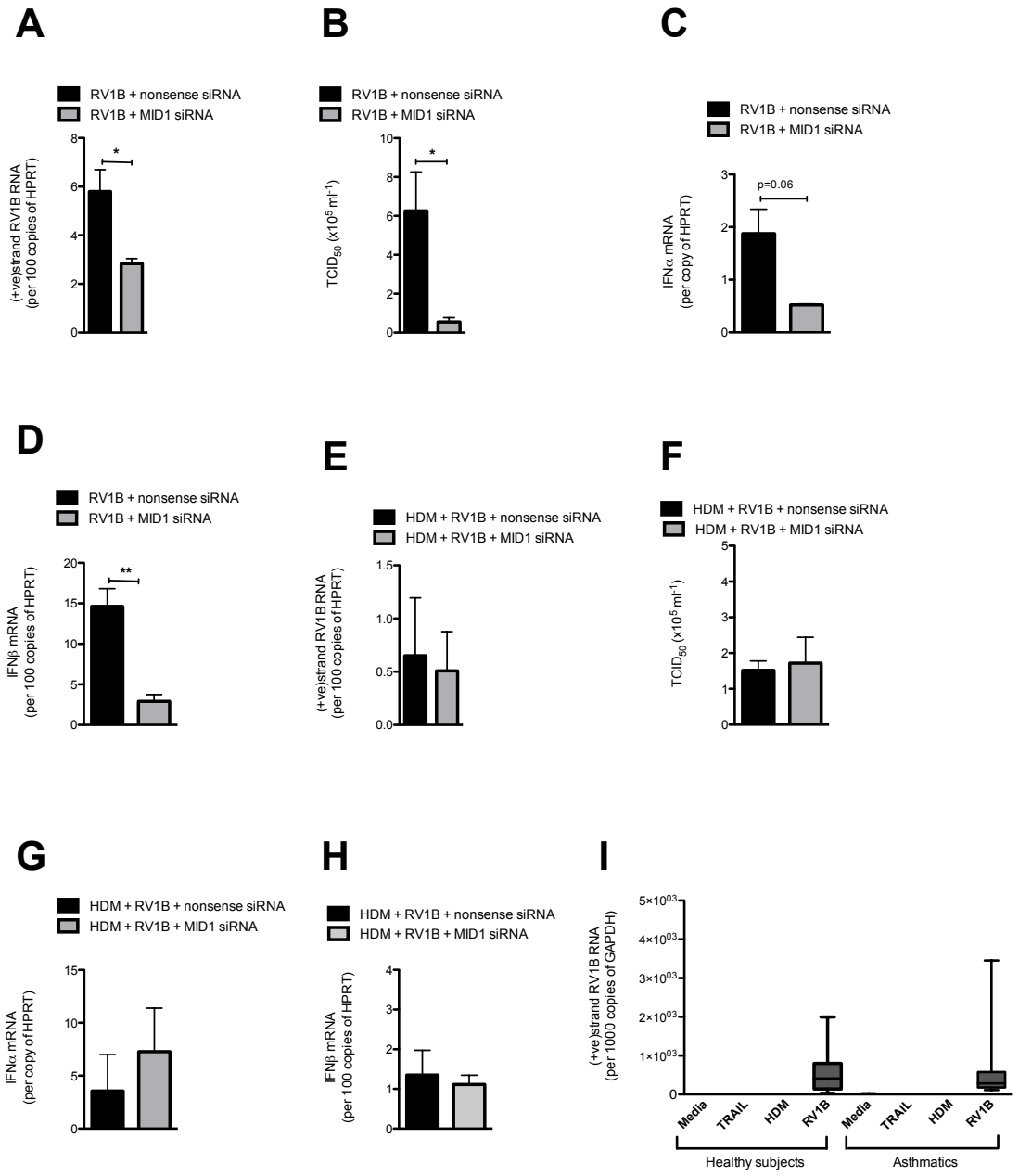

MID1 inhibition does not affect RV1B replication and IFN release in allergic mice. (**a**) Positive strand RV1B RNA, (**b**) RV1B titre, (**c**) IFNα and (**d**) IFNβ mRNA in the airway wall of naïve mice treated with a scrambled siRNA (nonsense siRNA) or a MID1 targeting siRNA (MID1 siRNA) 24hrs before RV1B challenge intranasally. (**e**) Positive strand RV1B RNA, (**f**) RV1B titre, (**g**) IFNα and (**h**) IFNβ mRNA in the airway wall of house dust mite allergic mice

treated with a scrambled siRNA (nonsense siRNA) or a MID1 targeting siRNA (MID1 siRNA) 24hrs before RV1B inoculation intranasally. (n=3-6 mice per group). (**i**) Positive strand RV1B RNA in primary airway epithelial cells from healthy subjects and asthmatics 24hrs after infection. Results are mean±s.e.m. *, $P < 0.05$, and **, $P < 0.01$.

Supplementary Fig 7

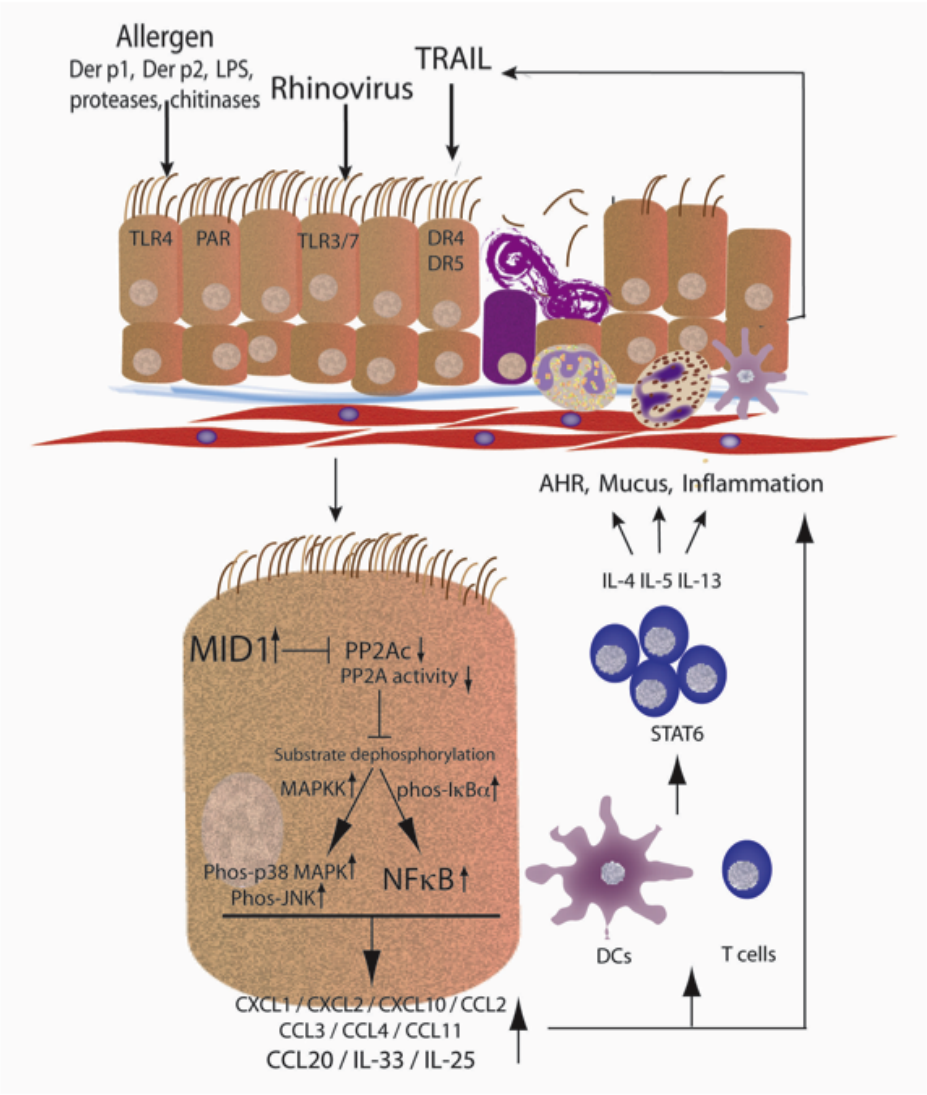

Proposed role of MID1 in allergic airways disease.

Supplementary Table 1 online**: Characteristics of healthy and asthmatic subjects.**

	Healthy	Asthmatic
N	14	14
Age (years)	53.7 (26, 82)	55.21 (38, 76)
Males, n (%)	9 (64.3)	2 (14.3)*
Non-smoker, n (%)	12 (85.7)	11 (78.6)
FEV_1% predicted	93.4 ± 4.0	75.9 ± 7.0*
ICS, n (%)	0 (0)	10 (71.4)
LABA, n (%)	0 (0)	10 (71.4)
OCS, n (%)	0 (0)	1 (7.1)

*, $P < 0.05$

Supplementary methods online**: Primer list.**

Mouse	*Forward*	*Reverse*
CCL5	GTGCCCACGTCAGGAGTAT	TCCTTCGAGTGACAAACACG
CCL17	AGTGGAGTGTTCCAGGGATG	CTGGTCACAGGCCGTTTTAT
CCL20	CGACTGTTGCCTCTCGTACA	AGGAGGTTCACAGCCCTTTT
CCL22	GACCTCTGATGCAGGTCCCTAT	GGATGTAGTCCTGGCAGCAGATA
GM-CSF	GCCATCAAGAAGCCCTGAA	GCGGGTCTGCACACATGTTA
HPRT	AGGCCAGACTTTGTTGGATTTGAA	CAACTTGCGCTCATCTTAGGCTTT
IFNα	GAACATCTTCACATCAAAGG	CAGAATGAGTCTAGGAGGGTTG
IFNβ	CTCCACGCTGCGTTCCTGCT	TCGGACCACCATCCAGGCGT
IL25	ATGTACCAGGCTGTTGCATTCTTG	CTAAGCCATGACCCGGGGCC
IL33	TCCTTGCTTGGCAGTATCCA	TGCTCAATGTGTCAACAGACG
MID1	CACTCGCTGAAGGAAAATGACCA	AATCCAAGGCAAAAGTGTCAAACG
Muc5AC	GCAGTTGTGTCACCATCATCTGTG	GGGGCAGTCTTGACTAACCCTCTT
TSLP	AGGCTACCCTGAAACTGAG	GGAGATTGCATGAAGGAATACC

Human	*Forward*	*Reverse*
CCL20	TGTGCTGTACCAAGAGTTTGCTCC	TCCAAGACAGCAGTCAAAGTTGCTT
GAPDH	ACAGTCAGCCGCATCTTCTTTTG	CCAATACGACCAAATCCGTTGAC
MID1	GTACACCATATTCACCGGACAAGC	AGTGGTTCTGCTTGATGTTGGGTA
TRAIL	TCGTGATCTTCACAGTGCTCCTG	ACAAGCAATGCCACTTTTGGAGTA
Virus	*Forward*	*Reverse*
RV1B	AGTCCTCCGGCCCCTGAATG	AAAGTAGTYGGTCCCATCCGC